Venting of Heat and Carbon Dioxide from Urban Canyons at Night

J. A. SALMOND* AND T. R. OKE

Department of Geography, University of British Columbia, Vancouver, British Columbia, Canada

C. S. B. GRIMMOND

Atmospheric Science Program, Department of Geography, Indiana University, Bloomington, Indiana

S. ROBERTS

Department of Geography, University of British Columbia, Vancouver, British Columbia, Canada

B. OFFERLE

Atmospheric Science Program, Department of Geography, Indiana University, Bloomington, Indiana, and Göteborg University, Göteborg, Sweden

(Manuscript received 25 July 2004, in final form 2 February 2005)

ABSTRACT

Turbulent fluxes of carbon dioxide and sensible heat were observed in the surface layer of the weakly convective nocturnal boundary layer over the center of the city of Marseille, France, during the Expérience sur Sites pour Contraindre les Modèles de Pollution Atmosphérique et de Transport d'Emission (ESCOMPTE) field experiment in the summer of 2001. The data reveal intermittent events or bursts in the time series of carbon dioxide (CO_2) concentration and air temperature that are superimposed upon the background values. These features relate to intermittent structures in the fluxes of CO_2 and sensible heat. In Marseille, CO_2 is primarily emitted into the atmosphere at street level from vehicle exhausts. In a similar way, nocturnal sensible heat fluxes are most likely to originate in the deep street canyons that are warmer than adjacent roof surfaces. Wavelet analysis is used to examine the hypothesis that CO_2 concentrations can be used as a tracer to identify characteristics of the venting of pollutants and heat from street canyons into the above-roof nocturnal urban boundary layer. Wavelet analysis is shown to be effective in the identification and analysis of significant events and coherent structures within the turbulent time series. Late in the evening, there is a strong correlation between the burst structures observed in the air temperature and CO_2 time series. Evidence suggests that the localized increases of temperature and CO_2 observed above roof level in the urban boundary layer (UBL) are related to intermittent venting of sensible heat from the warmer urban canopy layer (UCL). However, later in the night, local advection of CO_2 in the UBL, combined with reduced traffic emissions in the UCL, limit the value of CO_2 as a tracer of convective plumes in the UBL.

* Current affiliation: Division of Environmental Health and Risk Management, School of Geography Earth and Environmental Sciences, The University of Birmingham, Birmingham, United Kingdom.

Corresponding author address: J. A. Salmond, Division of Environmental Health and Risk Management, School of Geography Earth and Environmental Sciences, The University of Birmingham, Birmingham B15 2TT, United Kingdom.
E-mail: j.salmond@bham.ac.uk

1. Introduction

The thermal inertia, dryness, and roughness of urban surfaces are known to produce a weakly convective urban boundary layer (UBL) at night, at least at some densely developed sites (Uno et al. 1992; Casadio et al. 1996). This distinctly urban feature, which appears to be a weak form of the daytime convective boundary layer, is thought to be a product of the combined influences of increased mechanical turbulence resulting from the large surface roughness and thermal turbulence resulting from the urban heat island effect. Beyond such expectations, relatively little is known about urban turbulence at night or about the mechanisms that operate between the urban canopy layer (UCL) beneath the roof level and the UBL above. Progress toward improved understanding has been slow (Roth and Oke 1995), with very few field or modeling studies considering the processes involved.

Static stability over urban areas at night is less than in the surrounding countryside. This fact has been known for some time from measured temperature and wind profiles (e.g., Landsberg 1981; Oke 1995) and from more recent flux measurements (Christen and Vogt 2004; Grimmond et al. 2004). This weakly convective nocturnal urban boundary layer (NUBL) could be driven by several mechanisms. One is a simple upward heat flux from the warmer UCL. Observations of local-scale heat fluxes show the persistence of upward turbulent sensible heat flux well into, or even throughout, the night (Oke 1988; Grimmond and Oke 2002; Christen and Vogt 2004; Grimmond et al. 2004). The genesis of this effect is probably the release of sensible heat from storage in the urban fabric and, perhaps, from anthropogenic sources. A second mechanism is forwarded by Uno et al. (1988), who report a nocturnal convective layer driven by surface shear and the mechanical entrainment of sensible heat downward from an overlying inversion rather than encroachment.

Elucidating the importance of surface-generated convective processes relative to those associated with mechanical entrainment operating near the top of the UBL is beyond the scope of this study. The focus here is restricted to the potential role of street canyons as a source of convective plumes conveying heat from the UCL into the NUBL above.

Numerical and scale model studies of the daytime convective and neutral boundary layers suggest that vortex structures within street canyons are the main control on the exchange rate of pollutants with the UBL [e.g., between the canyon and the overlying atmosphere (Kastner-Klein and Plate 1999; Baik and Kim 2002; Britter and Hanna 2003)]. Even for this case, however, model and observational results suggest several complications, including the injection of turbulent structures from the convective mixed layer, the special effects of uneven roof levels and asymmetric canyons, thermal effects such as convective sheets rising along heated walls, and traffic turbulence (Kim and Baik 1999; Louka et al. 2000; Barlow and Belcher 2002; Britter and Hanna 2003).

The nocturnal case remains largely unresearched. Given that weak flow conditions are common at night, flow-driven vortex circulations are unlikely to be significant. On the other hand, because even small positive surface fluxes can be "sufficient to support convective motions in shallow boundary layers" (Casadio et al. 1996, p. 382), the release of heat stored in the urban fabric may be sufficient to support convective activity at night (Oke 1995). There is a large heat reservoir available in many densely built-up districts, where up to 50% of the daytime net radiation surplus may be stored in the urban fabric (Grimmond and Oke 2002). Urban surfaces within the UCL, such as canyon walls, may be inhibited from cooling at night because of their configuration, which favors shelter and gives them a relatively small view of the cold sky. Further, they may receive anthropogenic heat from the building interiors and, in the canyons, from vehicles, air conditioners, or leakage from buildings. The relative warmth of the canyons creates the potential for static instability, which may generate weak, intermittent convective activity (Oke 1995; Rotach 1995; Salmond et al. 2003).

Here we present a novel analytical technique, based on wavelet analysis, to examine patterns of turbulent transport through the urban surface layer at night by using observations of heat and carbon dioxide (CO_2) fluxes. Carbon dioxide is a comparatively inert gas and has merit as a tracer to identify turbulent transport processes operating between the UCL and NUBL above the city of Marseille, France. This merit is because of the relative absence of indoor heating or cooling or industrial emissions in the center of Marseille; CO_2 is primarily emitted at street level from vehicle exhausts. At night there may also be a small contribution from the respiration of vegetation, and this contribution is also mainly located in the UCL street canyons or courtyards (Grimmond et al. 2004). Through analysis of coherent structures within the NUBL just above the UCL, we identify signatures of CO_2 venting embedded in convective plumes emitted from street canyons.

There are many reasons why improved insight into nocturnal UCL–NUBL exchange is useful. Given the persistence of traffic emissions well into the night and the restricted horizontal dispersion found in sheltered canyons, there is a need to know the strength of vertical

transport between street canyons and the overlying urban boundary layer. Because vertical dispersion is also comparatively weak at night and is limited to only shallow depths (Godowitch et al. 1987; Rotach et al. 2004), we need to develop a process-based understanding of the temporal and spatial patterns in flux magnitude and direction across the top of the street canyons so as to develop better heat island models and to improve parameterization of urban surface–atmosphere interactions. This improvement, in turn, will enhance our ability to model and ultimately to predict characteristics of the UBL more accurately and to identify pollutant dispersion pathways more effectively.

2. Methods

a. Field observations

The data used were collected as part of the Expérience sur Sites pour Contraindre les Modèles de Pollution Atmosphérique et de Transport d'Emission (ESCOMPTE) field project undertaken in Marseille (Cros et al. 2004; Grimmond et al. 2004; Mestayer et al. 2005). Marseille (43.30°N, 5.40°E), the second largest city in France, is located on the Mediterranean Sea coast (Fig. 1). It is a major port, is the main industrial and commercial center for the Provence region, and has a metropolitan population of approximately two million people. The city is located in a region with a complex coastline and uneven terrain, and is surrounded by hills extending to 670 m above mean sea level (MSL).

The measurement site was located 70 m MSL in the old city center near "Vieux Port" (the old harbor) on the western seaboard of the region. This densely urbanized and comparatively homogenous district of the city largely consists of nineteenth-century residential and commercial buildings, approximately 4–6 storys in height, and extends approximately 2 km inland. There is little vegetation in the district [16% mean plan area (Grimmond et al. 2004)].

The area has narrow, irregularly oriented street canyons. Roads are paved with asphalt, and the building walls are up to 1 m thick and are typically constructed of limestone or granite. Roofs are covered with clay tiles or, less frequently, gravel (Roberts 2003). The mean building height is 16 m, and the mean width of streets is 7 m, giving a typical (height to width) aspect ratio of at least 2:1 [see Fig. 3 in Mestayer et al. (2005) for variability of heights].

b. Measurements

A pneumatic tower (Hilomast NX30) was installed on the roof of the 20-m-tall Cour d'Appel Administrative building (CAA; Fig. 1) (Cros et al. 2004; Grimmond et al. 2004). The tower was instrumented with radiation, micrometeorological, and standard meteorological instruments at two heights (Grimmond et al. 2004). Here we draw primarily on data from a Licor, Inc., LI-7500 infrared gas analyzer and an R.M. Young Company three-axis sonic anemometer, both of which are mounted at 43.9 m above ground level (AGL; i.e., about 24 m above the roof and 28 m above the mean roof level). Data were collected synchronously and stored at 10 Hz. Standard data processing and verification techniques were applied to the flux data as described in Grimmond et al. (2004). All times referred to herein are local daylight time (LDT).

Infrared radiation thermometers [Everest Interscience, Inc., Model 4000A or Model 4000.4GL (15° or 60° field of view, respectively)] were mounted to optimize the surface area "seen" by the sensor (Lagouarde et al. 2004). Roads oriented north–south and east–west, in the immediate vicinity of the tower, were sampled together with walls facing approximately north, south, east, and west. Clay tile roofs pitched at 17° facing in the four cardinal compass directions were also sampled to provide a weighted mean rooftop temperature. Data were sampled every 15 s, and means were recorded at 15-min intervals on Campbell Scientific, Inc., 21X or Onset Computer, Inc., HOBO dataloggers.

Here the focus is on nocturnal conditions, between sunset (~2100) and sunrise (~0600), during a period of anticyclonic weather between 23– and 27 June 2001 (yeardays 174–178). During this period, which was designated as an intensive observation period in the ESCOMPTE campaign, skies were cloudless with daytime sea-breeze circulations. On all four nights the prevailing wind flow at sunset was northwest, followed by a marked shift to southeast at 0230 LDT. Analysis of mesoscale model runs for the period shows no clear evidence for the development of a land breeze anywhere in Marseille (V. Masson 2003, personal communication). This shift is likely to be a response to local wind flows within the urban area resulting from the complex topography.

The mean wind speed at the site during the observations was less than 2 m s^{-1}, and the mean friction velocity was less than 0.3 m s^{-1}. Under these conditions shear turbulence across the top of the UCL is expected to be minimal. These are good conditions in which to identify the penetration of convective plumes from the UCL into the UBL.

The mean daytime energy balance observed during the period (Fig. 2) shows approximately 80% of the daily maximum available net radiation is partitioned directly into sensible heat fluxes—about 60% as the

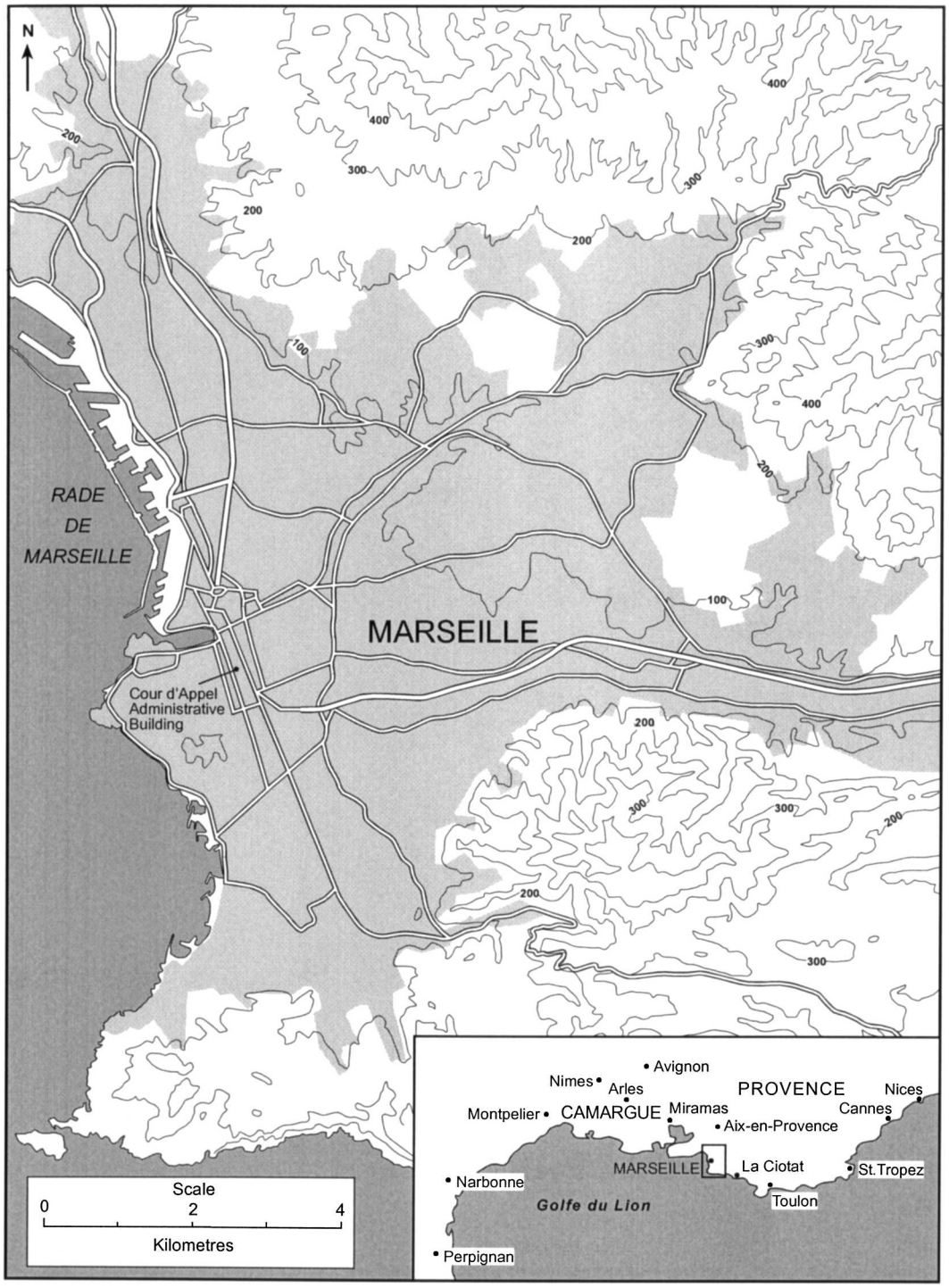

FIG. 1. Location of the instrumented tower at the Cour d'Appel Administrative building in Marseille and Marseille's location in southern France. Shaded areas are built up. North is to the top of each figure.

turbulent heat flux Q_H and about 20% as storage sensible heat flux (Grimmond et al. 2004). Turbulent heat flux remains positive throughout the full diurnal cycle. Although the small latent heat fluxes Q_E observed during the day are not surprising, given the lack of vegetation and the dry Mediterranean climate, the low ratio (2.6:1) of Q_H to the storage heat flux (ΔQ_S) was unexpected. It has been shown to be related to the wind

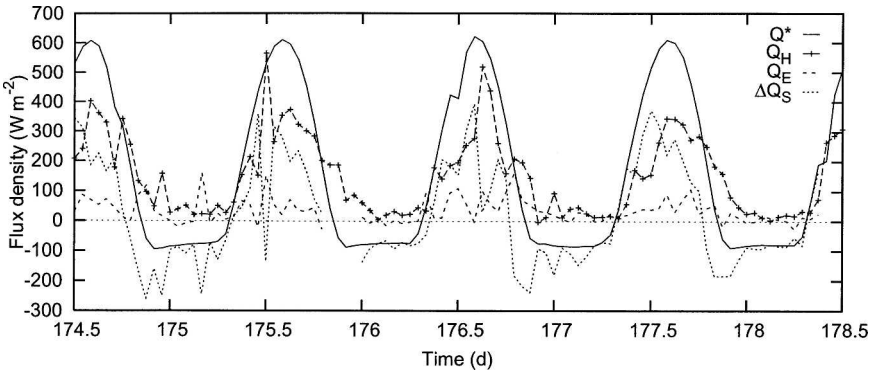

FIG. 2. Surface energy balance: net all-wave radiation (Q^*), turbulent sensible heat flux (Q_H), latent heat flux (Q_E), and storage heat flux (ΔQ_S, calculated as a residual) for the CAA site, using measurements at the height of 44 m AGL, for the period of 23–27 Jun 2001.

regime and the characteristics of the surface materials at this site (Roberts 2003).

Relative to other surface materials at this site, the roof tiles are unlikely to contribute significantly to positive sensible heat fluxes at night because they are made of clay, which has a low heat storage capacity; they are loosely attached, they have an attic space beneath giving good insulation, and their high albedo limits daytime heat absorption. In contrast, the thick stone walls in the deep canyons dominate the uptake of heat storage during the day, and it is available for release at night. The nature of the construction and structure of the street canyons is ideal for heat uptake. They have high thermal inertia and a large surface area and are dry. Further, their geometric form promotes multiple reflection of solar and infrared radiation, restricts the view of the cold-sky energy sink, and provides wind shelter.

The mean diurnal temperature regimes in Fig. 3 support this hypothesis. The ensemble mean diurnal surface temperature of two orthogonal street canyons, weighted by the fraction of surface area occupied by each canyon facet (walls and road), remains about 3°C warmer than the mean canyon air temperature throughout the night. By contrast, the mean surface temperature of the clay tile roofs drops below those of the canyon surfaces by 2200 LDT and below both the UCL and UBL air temperatures by 0100. Directly above the roofs there may be temporary inversions, but the temperature gradient between the UCL and UBL remains positive throughout the night.

c. Wavelet method

Wavelet analysis offers an alternative to traditional analytical tools, such as the Fourier transform, for the analysis of turbulence time series. It is a local, two-dimensional transform that facilitates the retention of information about the temporal location of frequencies within the dataset. The main use of wavelet analysis for the study of turbulence has been to detect and analyze coherent structures (Collineau and Brunet 1993; Irvine and Brunet 1996; Lohou et al. 2000; Scanlon and Albertson 2001). Coherent structures in velocity fields play an important role in flux transport. The presence of coherent structures in a dataset generates a form of local intermittency that is hard to quantify using a Fourier transform. Wavelet analysis, which encompasses many "desirable features of traditional conditional sampling" techniques (Hagelberg and Gamage 1994, p. 218), provides an objective means to define and quantify coherent structures within the time series.

So far "there is no consensus as to how hard one should work to choose the best wavelet for a given application and no firm guidelines about how to make such a choice" (Hubbard 1998, p. 88). In the absence of other criteria, Lau and Weng (1995, p. 2394) argue that the choice of a wavelet that bears the most "reasonable resemblance in form to the signal" will provide the most useful information from a wavelet transform. In this study we use the "Mexican hat" wavelet to objectively isolate and to quantitatively analyze coherent structures in the turbulent time series.

The Mexican hat wavelet (see Fig. 2 in Torrence and Compo, 1998) is symmetric and therefore coherent at the edge of any transition, effectively defining the start of the change in conditions (Hagelberg and Gamage 1994). The equation for the Mexican hat wavelet used here (for analysis of a time series x_n) is (Daubechies 1992)

$$\psi(x) = [(2/\sqrt{3})\pi^{-1/4}](1 - x^2)e^{-x^2/2}. \quad (1)$$

The characteristics of the Mexican hat wavelet can be

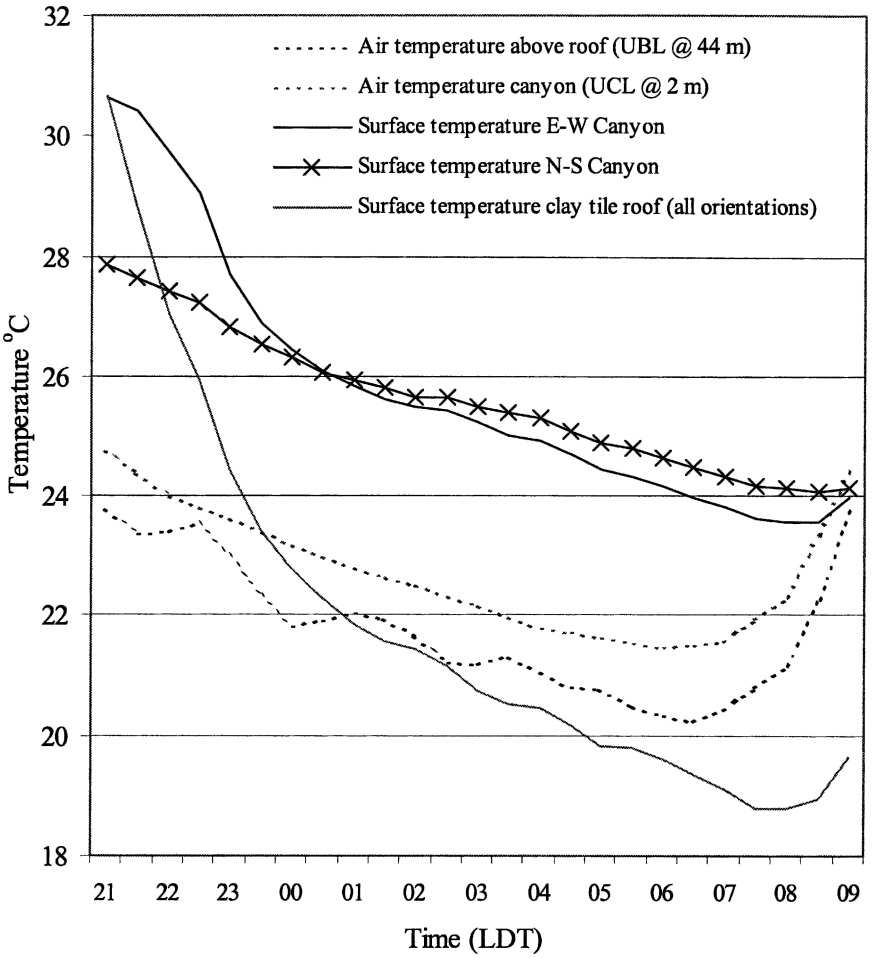

FIG. 3. Comparison of surface (infrared) temperatures for east–west- and north–south-oriented street canyons (average ensemble canyon temperature weighted according to the fraction of surface area occupied by each canyon component) and for clay tile roofs the mean air temperature in the canopy layer (2 m) and the urban boundary layer (44 m) in the period of 2–11 Jul 2001 (the only period for which data are available).

most effectively exploited to identify a jump or transition, because such changes are represented by a "zero crossing" in the wavelet coefficients at a scale that corresponds to the feature observed (Fig. 4). In this way the local timing, direction, and duration of events within the time series can be identified. However, the raw wavelet coefficients alone do not provide any information regarding the comparative significance of different events within the context of each individual time series.

The statistical significance of the wavelet coefficients is assessed here using a 95% confidence interval. The test is wavelet specific and uses the autocorrelation (at lag $= -1$) of the time series to generate a theoretical red-noise spectrum that is specific to each time series (Torrence and Compo 1998). This procedure, originally developed for stationary signals, is based on the assumption that the variance and covariance of the dataset have a chi-square distribution (almost certainly violated for atmospheric turbulence data). However, the test has been successfully applied by Galmarini and Attie (2000), Attie and Durand (2003), and Salmond (2005) to reveal interesting spatial and temporal patterns embedded within atmospheric turbulence time series and insight into the data.

In Fig. 4c the test is applied to the square of the wavelet coefficients corresponding to the scale of the structures observed in the test time series shown in Fig. 4a. Using this technique, it is then possible to identify the significant structures within a time series, which, in the context of atmospheric turbulent transport, are likely to be those structures primarily responsible for the transport of atmospheric pollutants.

For the purposes of this paper the Mexican hat wave-

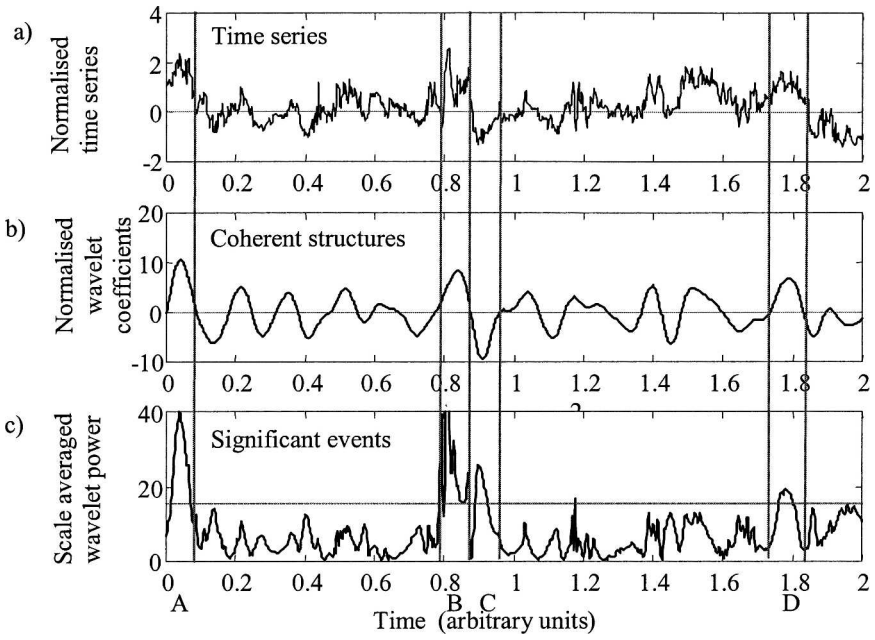

FIG. 4. An example of (a) a turbulent time series, and the associated (b) coherent structures and (c) significant events as determined following Torrence and Compo (1998). Four significant events are identified (A–D). By comparing these with the relevant coherent structures, three of these (A, B, and D) are seen to be associated with a positive deviation or structure and C is seen to be associated with a negative deviation or structure. Zero-crossing points in the coherent structures correspond well to the start and end of the relevant event in the time series.

let is first applied to 30-min time series that have been normalized by dividing each series by its standard deviation. The continuous form of the wavelet transform [the code for the basic Mexican hat wavelet transform was modified from Torrence and Compo (1998; available online at http://paos.colorado.edu/research/wavelets/ as of January 2002)] of a time series x_n (Torrence and Compo 1998) is

$$W_n(s) = \sum_{n'=0}^{N-1} x_{n'} \psi^* \left[\frac{(n' - n)\delta t}{s} \right], \quad (2)$$

where $\psi^*(t)$ is the complex conjugate of the wavelet function (normalized to have unit energy) for time step δt, s is the "dilation" parameter used to change the scale, n is the translation parameter used to slide in time; and n' indicates the index over which the equation is summed.

The Mexican hat wavelet was applied to the time series using a discrete set of 13 scales of fractional powers of two:

$$s_j = s_o 2^{j\delta j}, \quad (3)$$

where $s_o = 0.2$ s and $\delta j = 0.5$. After the effects of padding the time series have been taken into account, this gives a range of valid scales between 0.2 and 2048 s (~34 min).

3. Results

a. Wavelet analysis of turbulent time series

Examination of the 10-Hz nocturnal turbulence data shows intermittent "spikes" in CO_2 concentration, superimposed upon a more stable mean background value (Fig. 5). Note here we use the term spikes to refer to a marked excursion in the time series. Detailed analysis of the coherent structures shows that these spikes are consistent with sudden jumps or bursts in the time series.

Visual inspection shows that spikes identified in the CO_2 time series are correlated with similar features in the temperature time series. This correlation may indicate convective plumes emanating from the street canyons. However, to develop a process-based understanding of these events and to explore the hypothesis of canyon venting, a more thorough analysis of these features across the whole dataset is required.

Figure 6b is a scalogram that illustrates the square of the wavelet coefficients for a typical time series of CO_2 concentration calculated using the Mexican hat wave-

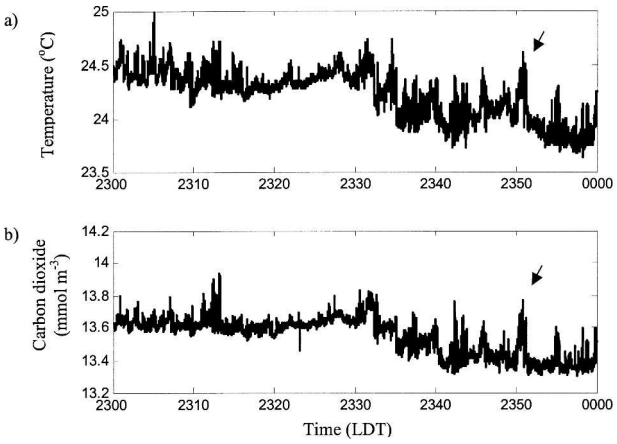

FIG. 5. Time series showing (a) temperature and (b) carbon dioxide fluctuations for 2300–0000 LDT 26 Jun 2001. Arrows point to an example of a spike identified in each time series.

let. The lightest areas (white) indicate a high degree of correlation between the wavelet and the time series. The "cone of influence" (the area below which data are considered unreliable) is also marked. Wavelet coefficients that are statistically significant are contoured in black. Because of the high temporal resolution of the scalogram, the contours appear as black lines at small scales. Wavelet analysis identifies the presence and temporal location of significant structures within a time series. Intermittent periods of significant activity at turbulent scales ($<2^3 = 8$ s) correspond well with the observed bursts of CO_2. This correspondence is a consistent feature of the dataset.

To examine these scales more effectively, the scale average of the wavelet power at scales of less than 8 s (the scales at which the largest proportion of significant structures is found) is calculated and is compared with the calculated red-noise spectra assessed at the 95% significance level. Averaging over this range of scales limits the effects of instrumental noise. The process is repeated for the temperature and vertical velocity time series to ascertain the characteristics of the relations between the scalar variables at these scales. The purpose of this analysis is to identify significant structures in the time series that are likely to correspond to important pollutant or energy transport events. For example, four significant spikes of CO_2 are identified in this way in Fig. 6c by the letters A–D.

Figure 7 illustrates the temporal relation between the significant events observed in the CO_2 and the temperature and vertical velocity time series identified at scales of less than 8 s. There is good synchronicity (cor-

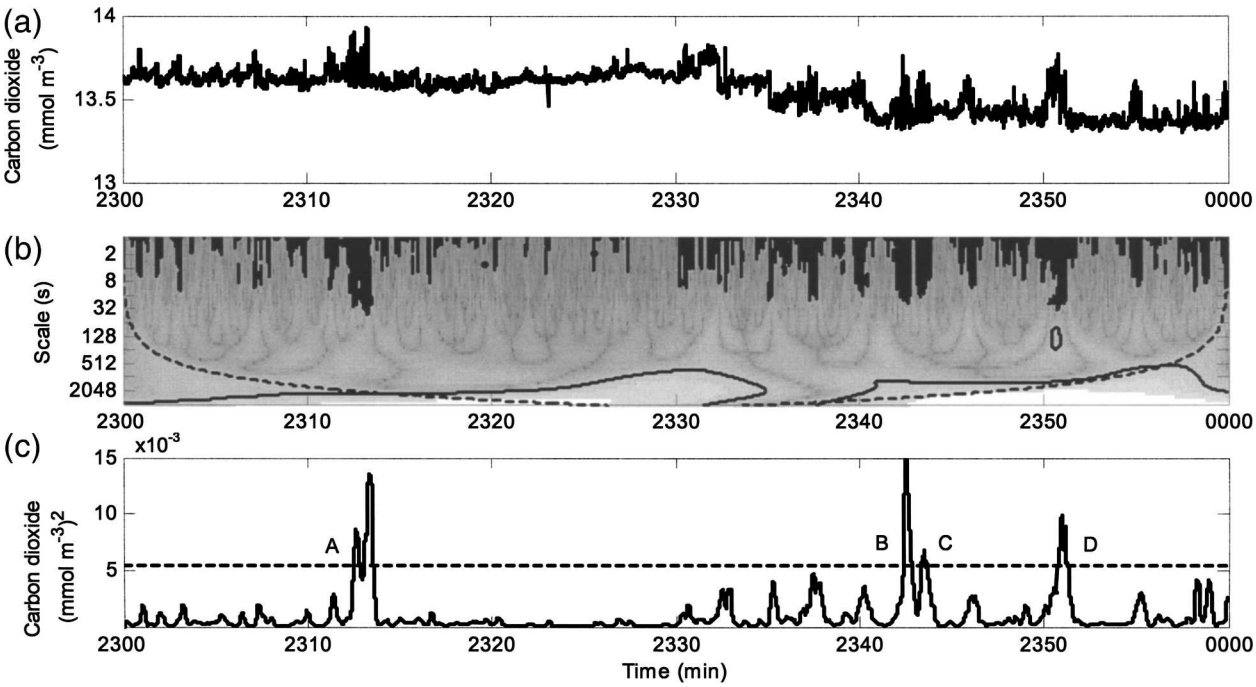

FIG. 6. (a) CO_2 time series, (b) scalogram and (c) scale-averaged wavelet power (and significance level, dashed line) for scales <8 s for 2300–0000 LDT 26 Jun 2001. Four spikes identified are labeled A–D. Using this information alone leaves subjectivity regarding the definition of one spike as shown in Fig. 8c, identified at point A, and two spikes at points B and C. To resolve it, the spikes are identified using the zero-crossing points of the coherent structures (see Fig. 4). This approach clarifies that A is a single spike, whereas B and C are two separate structures. See text for further explanation.

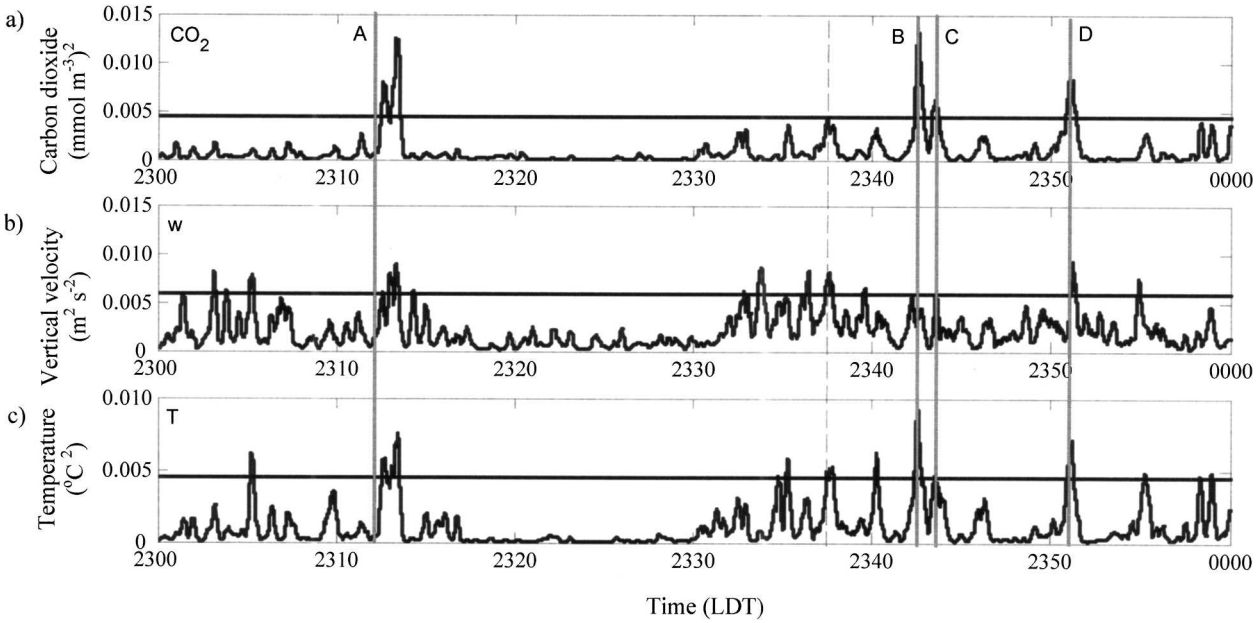

FIG. 7. Scale-averaged wavelet power (and significance level, horizontal dashed line) for (a) carbon dioxide, (b) vertical velocity, and (c) temperature for scales <8 s for 2300–0000 LDT 26 Jun 2001. Vertical lines link coherent structures in the three variables (see text). Letters A–D identify significant structures in CO_2.

relation coefficient $r = 0.77$) between the CO_2 spikes and similar structures in the temperature time series (solid vertical lines). Comparison of Figs. 7a and 7b indicates that there is less correlation between the significant events in the vertical velocity time series and those in CO_2 ($r = 0.44$). Further, the events are not preceded by any significant structures in the vertical velocity time series. This result suggests that these events may be driven more by convective processes than by mechanical processes.

Although Fig. 7 gives some information about the main structures in the time series, it does not provide details regarding the nature of the underlying process. For example, it is not possible to identify whether the significant spikes represent an increase or decrease in temperature (or CO_2) or whether they are associated with positive or negative vertical velocity structures. To get this kind of information from wavelet analysis it is necessary to return to the original wavelet coefficients and extract characteristics of coherent structures.

Normalized wavelet coefficients corresponding to a scale of 8 s are extracted (Fig. 8), which gives information about the direction of observed changes in the original time series at 8 s. By combining the information in Figs. 7 and 8 the direction of flow associated with significant structures can be determined. Indeed, it is possible to ascertain that the dominant spikes of CO_2 are representative of localized *increases* in concentration and that they are associated with localized *increases* in temperature. It is also possible to determine that these bursts typically coincide with updrafts.

However, Fig. 7 also reveals a number of significant structures in the temperature time series that are not matched by similar structures in CO_2 (see the vertical dashed line). For example, between 2330 and 2340, three spikes in temperature are observed without coincident significant bursts in CO_2. Figure 8 shows that these spikes coincide with downdrafts and that they actually represent localized periods of *decreased* temperature, indicating a downward vertical transport of cooler air from above. The absence of corresponding significant "clean-air structures" in the CO_2 time series suggests that, unlike between the UCL and UBL, there is a minimal gradient in CO_2 concentration in the UBL.

To examine the characteristics of energy and pollutant transfer from the UCL to the UBL, the characteristics of the significant structures associated with each of the three variables (CO_2, temperature, and vertical velocity) are examined in detail throughout the four nights. All three time series are analyzed to provide consistent evidence for any venting processes and to ensure that the majority of events coupling the UCL to the UBL are identified. For example, cases in which warm air parcels with high concentrations of CO_2 are observed to coincide with an updraft are highly likely to represent the intermittent ejection of air from the street canyon. However, because the technique relies on a gradient in the variable for a significant structure to be

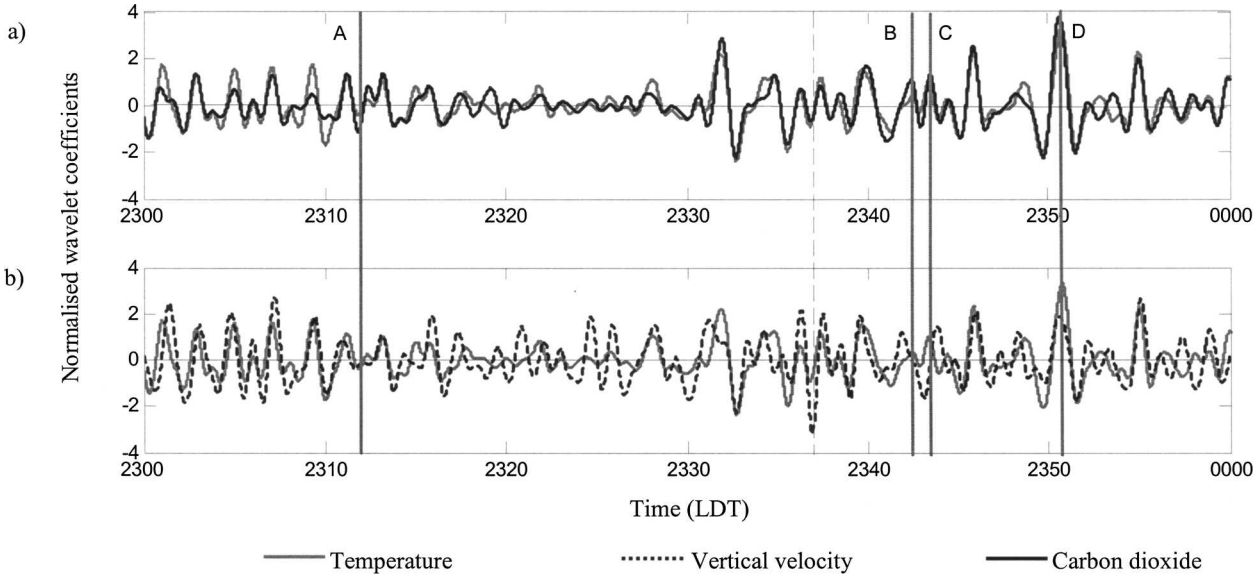

FIG. 8. Coherent structures in wavelet coefficients for (a) carbon dioxide and air temperature and (b) air temperature and vertical velocity time series at 8-s scale for 2300–0000 LDT 26 Jun 2001. Vertical lines link coherent structures in the three variables (see text). Letters A–D identify significant structures in CO_2 (see Fig. 7).

observed, it is possible that the number and timing of significant events between the time series vary. For example, Louka et al. (2000) note that the intermittent "flapping" of the shear layer may trigger ejection events. Thus, although it is most likely that warm parcels with high concentrations of CO_2 are ejected from the street canyon, it is also possible that a mechanical sweep from shear layer instability results in the ejection of thermally neutral and/or clean air, depending on the timing of the event. The analysis of both temperature and CO_2 concentrations therefore not only provides increased evidence for pollutant venting but may also yield further information about the underlying nature of the processes involved.

b. Nocturnal convective regimes

During the four nights analyzed, 132 significant spikes in CO_2 concentration, 212 similar spikes in temperature T, and 148 spikes in vertical velocity w were observed (Table 1). These events had mean durations of 81 (CO_2), 52 (T), and 120 (w) s, respectively. Throughout these nights the dominant significant structures identified in all three time series are associated with upward movement of warm air with high concentrations of CO_2 (Table 2, lines in boldface type). No relation could be identified between either the number or the duration of CO_2 spikes and the mean wind speed (as observed in the UBL). This strongly supports the hypothesis that these events represent air ejected from street canyons.

However, a smaller proportion of the updraft structures are associated with warm, clean (low CO_2) air (Table 2). Thus, it appears that the correlation between CO_2 and T is not as robust an indicator of street canyon venting as anticipated from Figs. 7 and 8. Indeed, the overall correlation across the whole dataset between the significant structures in the two time series is $r = 0.3$. Analysis of 1) the temporal variation of the correlation between these two variables throughout the nocturnal period and 2) the variations in the number of significant CO_2 events observed (Fig. 9) suggest that the presence of two distinct regimes operating during the night may account, in part, for the poor correlations observed.

1) POLLUTANT VENTING FROM STREET CANYONS: 2200–0130

Between 2200 and 0130 LDT, spikes in CO_2 concentration are consistently observed within the dataset.

TABLE 1. Total number of significant structures identified during the 4-day period, between 2200 and 0130, and between 0130 and 0600 LDT for the carbon dioxide, temperature, and vertical velocity time series.

	No. of structures identified		
	All data	2200–0130	0130–0600
CO_2	132	73	59
T	212	81	131
w	148	72	76

TABLE 2. Percentage of significant structures characterized by updrafts and downdrafts, warming/cooling, and increased/decreased CO_2 for the carbon dioxide and temperature time series during all four nights observed. See text for explanation of boldface rows.

		Updrafts				Downdrafts			
	Period	Warm, increased CO_2	Warm, decreased CO_2	Cool, increased CO_2	Cool, decreased CO_2	Warm, increased CO_2	Warm, decreased CO_2	Cool, increased CO_2	Cool, decreased CO_2
CO_2	All	**36.0**	**10.6**	**2.9**	**4.6**	**8.9**	**5.6**	**13.0**	**18.4**
	2200–0130	59.0	1.3	4.3	8.1	11.4	0.9	3.8	11.2
	0130–0060	18.1	17.7	1.9	1.9	6.9	9.3	20.2	24.0
T	All	**45.4**	**17.8**	**3.8**	**7.3**	**9.1**	**6.3**	**4.3**	**6.0**
	2200–0130	49.0	7.3	5.1	11.0	9.6	2.7	2.1	13.2
	0130–0600	42.2	26.1	2.8	4.6	8.8	9.1	5.9	0.5

During this period there is also a strong correlation between temperature and CO_2 (Fig. 9). Detailed analysis of the coherent structures of the significant events in this period reveals that the dominant structures observed in both time series are positive spikes (i.e., increased CO_2 concentration and warmer air) and are associated with updrafts (Table 2). This result strongly suggests that in this period pollutant and heat exchange from the street canyon dominate the turbulent transport.

Of interest is that, although roof surface temperatures remain above the mean air temperature of the UBL, we see few examples (7%) of warm air updrafts associated with low CO_2 concentrations. These would be indicative of convective updrafts that do not penetrate into the UBL (Table 2). The analysis also shows the existence of a small number of events associated with the upward motion of cool air. In these cases, the temperature gradient is very small. This phenomenon requires further investigation.

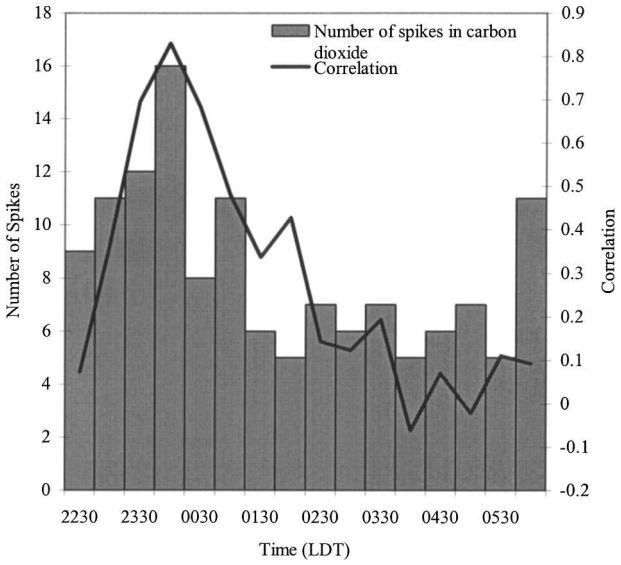

FIG. 9. Mean number of spikes identified (gray bars) and the correlation (black line) between air temperature and CO_2 time series at scales <8 s, between 2230 and 0600 LDT for 23–27 Jun 2001.

2) CO_2 ADVECTION ALOFT: 0130–0500

Between 0130 and 0500, the CO_2 spikes occur more intermittently, are fewer in number, and no longer coincide with similar features in the temperature time series (Figs. 9 and 10). Further, the correlation between the structures observed at scales of less than 8 s in the temperature and CO_2 time series drops significantly (Fig. 9 and Fig. 11a). During this period, updrafts associated with warm CO_2-rich air no longer dominate the structures observed in the CO_2 time series (Table 2). Instead, updrafts associated with warm air with both high and low CO_2 concentrations are equally as important as downdrafts of cool air with high and low CO_2 concentrations. In comparison, more than 60% of the significant structures in the temperature time series represent updrafts of warm air. This suggests that after 0130 either the CO_2 and temperature spikes are responding to different underlying processes or the absence of a clear vertical gradient in CO_2 limits the use of this gas as an effective tracer.

Between 0130 and 0230, data from the sonic anemometer mounted at 44 m MSL (and thus representative of flows in the UBL at this site) consistently reveal a shift in the mean wind direction from northwest to southeast (see Fig. 12b). Hence, the flow changes from a fetch that may include the Vieux Port to a city fetch that may be influenced by drainage flows from the hills (Fig. 1). Analysis of the mean CO_2 concentration in the UBL (Fig. 12a) shows that the ~180° change in wind direction is associated with a marked increase in mean CO_2 concentration of 1.5 mmol m^{-3}. This increase may be due to the longer urban fetch from the southeast or to advection of a local plume of CO_2 over the site. The UCL–UBL gradient of CO_2 is also re-

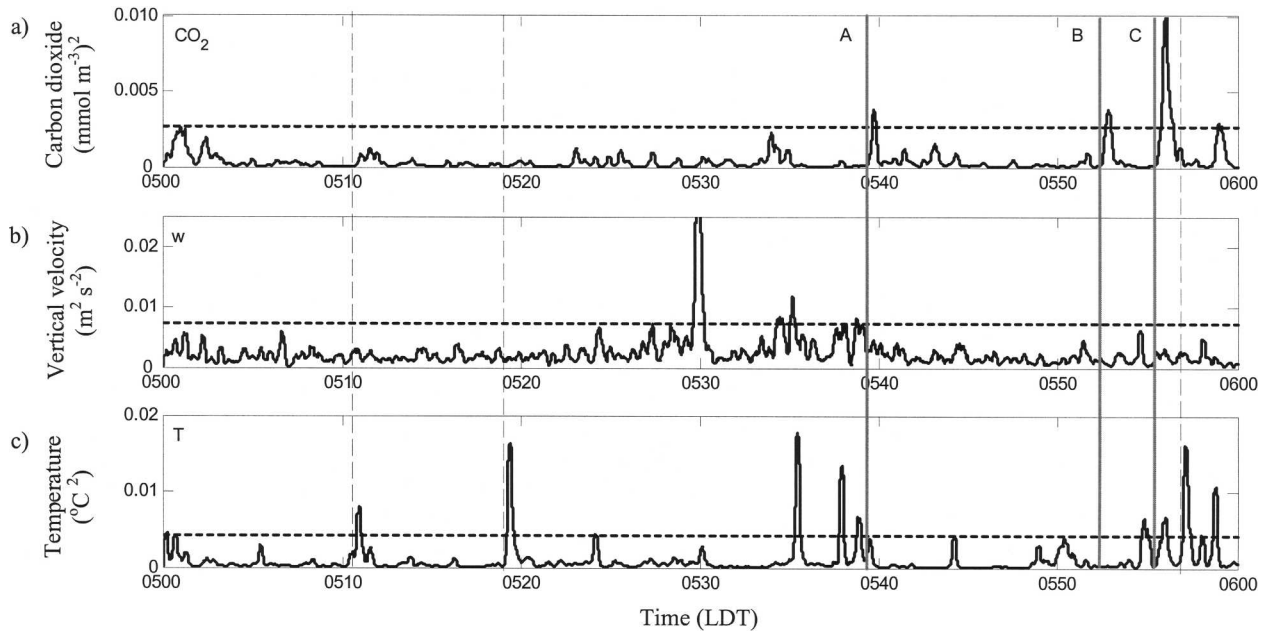

FIG. 10. Scale-averaged wavelet power (and significance level, horizontal dashed line) for (a) carbon dioxide, (b) vertical velocity, and (c) air temperature for scales <8 s for 0500–0600 LDT 27 Jun 2001. Letters A–C identify significant structures in CO_2.

duced by this increase in the UBL. It may also be affected by the fact that traffic sources in the UCL are reduced at this time of night.

The increase in the UBL concentration of CO_2 is considerably greater than the small increases in concentration observed within each localized spike in the time series (0.12 mmol m^{-3}). The changes in the gradient between the two levels affect the number of events detected. For example, comparison of Figs. 10 and 11a shows that the significant CO_2 structures observed in the later period are bursts of cleaner air (decreased concentration), rather than localized plume-induced increases. Given the 1.4°C difference between the UCL and UBL at this time, we might expect to see a negative correlation between the two variables in any convective plumes from the UCL. There is only a weak positive correlation between significant coherent structures in CO_2 and temperature, and clean-air bursts are some-

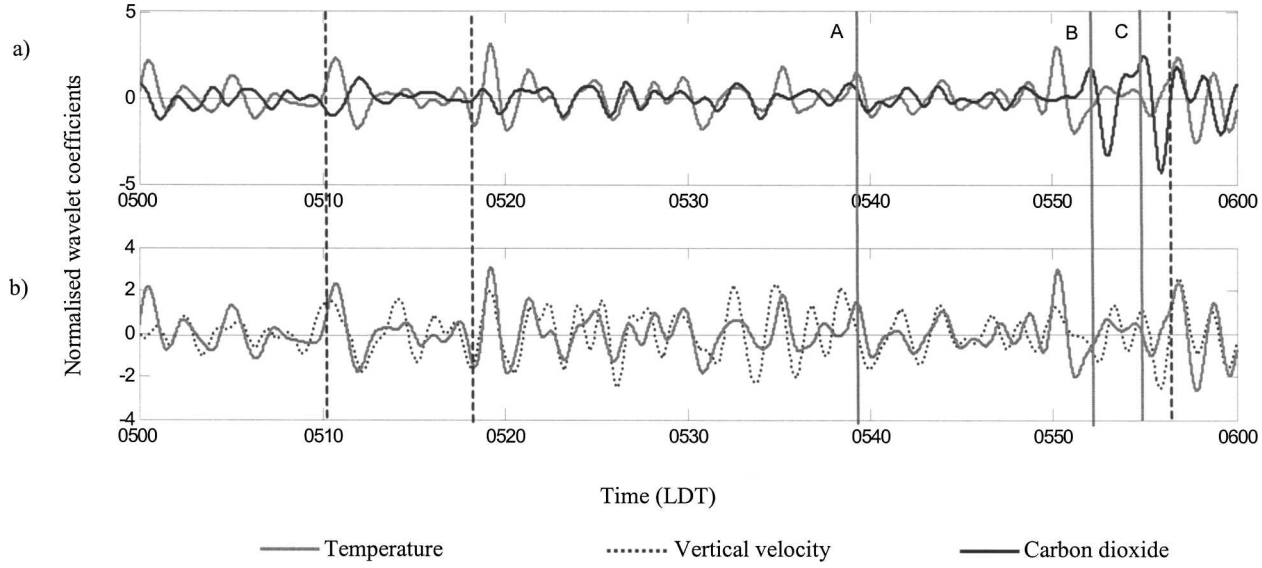

FIG. 11. Coherent structures in wavelet coefficients for (a) carbon dioxide and air temperature and (b) air temperature and vertical velocity time series at 8-s scale for 0500–0600 LDT 27 Jun 2001. Letters A–C identify significant structures in CO_2 (see Fig. 10).

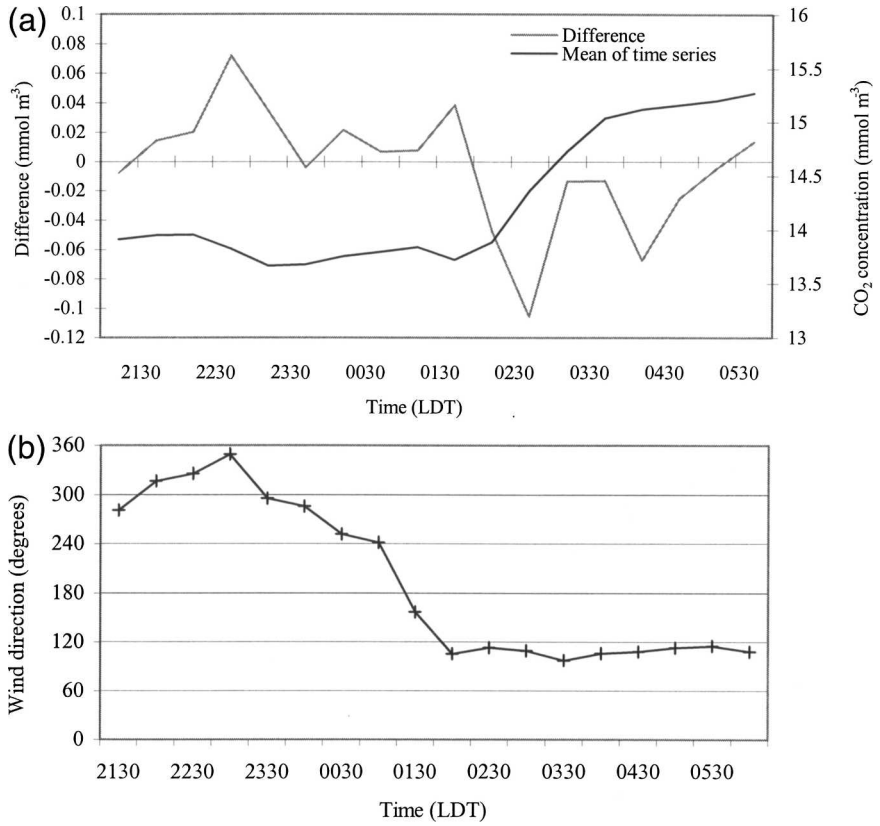

FIG. 12. (a) Mean CO_2 concentration and the difference between the CO_2 concentration in spikes and the mean of the time series. (b) Mean wind direction for 2130–0730 LDT for 23–27 Jun 2001.

times associated with downdrafts rather than updrafts (Fig. 11). So the observed CO_2 structures are equally likely to be downward entrainment of air from aloft as they are to be convective plumes from the UCL.

It is interesting that the number of spikes observed in the temperature time series increases in this part of the night (Table 1) and that there is only a small increase in the relative importance of warm downdrafts (Table 2). Given the consistent gradient in temperature between the UCL and UBL and given that by that time roof surface temperatures have dropped below the UBL air temperature (Fig. 3), the dominant thermal structures are still likely to originate as convective plumes from the street canyons. However, without the use of CO_2 as a tracer, it is difficult to differentiate between plumes from the UCL and turbulent structures limited to the UBL.

c. *Evidence for entrainment of heat from the UBL to the surface*

Throughout the four-night observation period, evidence for the entrainment of sensible heat from aloft was minimal. Warm plumes associated with downdrafts typically accounted for less than 16% of the structures observed in the temperature time series. This view is further supported by the analysis of coherent structures at all scales, which shows weak positive correlation between the temperature and vertical velocity time series ($r = 0.5$). Thus, the evidence suggests that although mechanical turbulence may exist at the top of the UBL and the subsequent decrease in stability may enhance convective heat loss from the surface, the entrainment of warm air from aloft is not an important source of heat energy for the UBL of Marseille. It is likely, therefore, that the convective characteristics of the nocturnal UBL are primarily due to convective heat loss from street canyons, as intermittently vented plumes.

4. Conclusions

Formulation of a general approach to identify and characterize the turbulent transport of energy and pollutants within the urban canopy layer, and between the canopy layer and the overlying urban boundary layer, is

considered problematic (Kastner-Klein and Plate 1999). The present study shows that wavelet analysis can be used to identify significant coherent structures in turbulent time series and can provide insight into the processes operating in the urban nocturnal boundary layer. Significant spikes in temperature, CO_2 concentration, and vertical velocity are seen throughout the turbulent time series observed at night over a densely built-up site in Marseille. During the late evening hours there is a strong correlation between the atmospheric structures observed in the temperature and CO_2 time series at turbulent scales. Analysis of the relevant coherent structures suggests that the bursts of CO_2 observed in the UBL are related to intermittent venting of sensible heat from the warmer urban canopy layer. However, later in the night, the reduced gradient in CO_2 concentrations with height, perhaps resulting from local advection of CO_2 within the UBL and/or reduced traffic emissions in the UCL, limits the value of CO_2 as a tracer of convective plumes in the UBL.

Nevertheless, evidence from the temperature time series indicates that convective plumes continue throughout the night. This result is probably related to the persistent release of stored heat from the canyons (Fig. 2). The absence of evidence of vertical entrainment of sensible heat from above the UBL supports the notion that these convective structures from the street canyons play an important role in maintaining the convective characteristics of the nocturnal UBL.

The importance of these processes is reflected in an increasing number of papers that highlight the need for enhanced understanding of the turbulent transport processes operating both within and above the street canyon (Gerdes and Olivari 1999; Pavageau and Schatzmann 1999; Baik and Kim 2002). There are indications that these processes may be fundamental to a comprehensive understanding (and ultimately prediction) of pollutant dispersion and should not be ignored in the development of future urban- and regional-scale air-quality models (Kastner-Klein and Plate 1999). The results imply that, in addition to CO_2, pollutants associated with vehicle exhaust may also build up within dense urban canyons, leading to high concentrations over short time periods. The application of wavelet analysis to richer datasets, which include vertical profiles of temperature and pollutants through the UCL and UBL, might enable further insights into the processes driving turbulence in the nocturnal UBL.

Acknowledgments. We extend thanks to Drs. Joel Noilhan and Valery Masson of Météo France, to Phoebe Jackson and Cindy Walsh for field assistance, to members of the ESCOMPTE project team who provided forecasts, and to the President of the Cours Administrative d'Appel for access to the observation site. This research was supported by funds from the Canadian Foundation for Climate and the Atmospheric Sciences (TO; GR22), the Natural Sciences and Engineering Research Council of Canada (TO), the Conseil National de Recherche Scientifique of France (SG, TO), and the National Science Foundation (SG; BCS-0095284).

REFERENCES

Attie, J.-L., and P. Durand, 2003: Conditional wavelet technique applied to aircraft data measured in the thermal internal boundary layer during sea-breeze events. *Bound.-Layer Meteor.,* **106,** 359–382.

Baik, J. J., and J. J. Kim, 2002: On the escape of pollutants from urban street canyons. *Atmos. Environ.,* **36,** 527–536.

Barlow, J. F., and S. E. Belcher, 2002: A wind tunnel model for quantifying fluxes in the urban boundary layer. *Bound.-Layer Meteor.,* **104,** 131–150.

Britter, R. E., and S. R. Hanna, 2003: Flow and dispersion in urban areas. *Annu. Rev. Fluid Mech.,* **35,** 469–496.

Casadio, S., A. DiSarra, G. Fiocco, D. Fua, F. Lena, and M. P. Rao, 1996: Convective characteristics of the nocturnal urban boundary layer as observed with Doppler sodar and Raman lidar. *Bound.-Layer Meteor.,* **79,** 375–391.

Christen, A., and R. Vogt, 2004: Energy and radiation balance of a central European city. *Int. J. Climatol.,* **24,** 1395–1421.

Collineau, S., and Y. Brunet, 1993: Detection of turbulent coherent motions in a forest canopy part 1: Wavelet analysis. *Bound.-Layer Meteor.,* **65,** 375–379.

Cros, B., and Coauthors, 2004: The ESCOMPTE program: An overview. *Atmos. Res.,* **69,** 241–279.

Daubechies, I., 1992: *Ten Lectures on Wavelets*. CBMS-NSF Regional Conference Series in Applied Mathematics, Vol. 61, SIAM, 357 pp.

Galmarini, S., and J.-L. Attie, 2000: Turbulent transport at the thermal inertial boundary layer top: Wavelet analysis of aircraft measurements. *Bound.-Layer Meteor.,* **94,** 175–196.

Gerdes, F., and D. Olivari, 1999: Analysis of pollutant dispersion in an urban street canyon. *J. Wind Eng. Ind. Aerodyn.,* **82,** 105–124.

Godowitch, J. M., J. K. S. Ching, and J. F. Clarke, 1987: Spatial variation of the evolution and structure of the urban boundary layer. *Bound.-Layer Meteor.,* **38,** 249–272.

Grimmond, C. S. B., and T. R. Oke, 2002: Turbulent heat fluxes in urban areas: Observations and a local-scale urban meteorological parameterization scheme (LUMPS). *J. Appl. Meteor.,* **41,** 792–810.

——, J. A. Salmond, T. R. Oke, B. Offerle, and A. Lemonsu, 2004: Flux and turbulence measurements at a dense urban site in Marseille. *J. Geophys. Res.,* **109,** D24101, doi:10.1029/2004JD004936.

Hagelberg, C. R., and N. K. K. Gamage, 1994: Structure-preserving wavelet decompositions of intermittent turbulence. *Bound.-Layer Meteor.,* **70,** 217–246.

Hubbard, B. B., 1998: *The World According to Wavelets: The Story of a Mathematical Technique in the Making*. 2d ed. A. K. Peters, 330 pp.

Irvine, M. R., and Y. Brunet, 1996: Wavelet analysis of coherent

eddies in the vicinity of several vegetation canopies. *Phys. Chem. Earth,* **21,** 161–165.

Kastner-Klein, P., and E. J. Plate, 1999: Wind-tunnel study of concentration fields in street canyons. *Atmos. Environ.,* **33,** 3973–3979.

Kim, J. J., and J. J. Baik, 1999: A numerical study of thermal effects on flow and pollutant dispersion in urban street canyons. *J. Appl. Meteor.,* **38,** 1249–1261.

Lagouarde, J.-P., P. Moreau, M. Irvine, J.-M. Bonnefond, J. A. Voogt, and F. Sollie, 2004: Airborne experimental measurements of the angular variations in surface temperature over urban areas: Case study of Marseille (France). *Remote Sens. Environ.,* **93,** 443–462.

Landsberg, H. E., 1981: *The Urban Climate*. Academic Press, 275 pp.

Lau, K.-M., and H. Weng, 1995: Climate signal detection using wavelet transform: How to make a time series sing. *Bull. Amer. Meteor. Soc.,* **76,** 2391–2402.

Lohou, F., A. Druilhet, B. Campistron, J. L. Redelspergers, and F. Said, 2000: Numerical study of the impact of coherent structures on vertical transfers in the atmospheric boundary layer. *Bound.-Layer Meteor.,* **97,** 361–383.

Louka, P., S. E. Belcher, and R. G. Harrison, 2000: Coupling between air flow in streets and the well developed boundary layer aloft. *Atmos. Environ.,* **34,** 2613–2621.

Mestayer, P. G., and Coauthors, 2005: The Urban Boundary Layer field campaign in Marseille (UBL/CLU-ESCOMPTE): Set-up and first results. *Bound.-Layer Meteor.,* **114,** 315–365.

Oke, T. R., 1988: The urban energy balance. *Prog. Phys. Geogr.,* **12,** 471–508.

——, 1995: The heat island of the urban boundary layer: Characteristics, causes and effects. *Wind Climate in Cities*, J. E. Cermak et al., Eds., Kluwer Academic, 81–107.

Pavageau, M., and M. Schatzmann, 1999: Wind tunnel measurements of concentration fluctuations in an urban street canyon. *Atmos. Environ.,* **33,** 3961–3971.

Roberts, S. M., 2003: Heat storage in a densely-built Mediterranean city centre. M.Sc. thesis, Atmospheric Science Programme, Department of Geography, University of British Columbia, 154 pages.

Rotach, M. W., 1995: Profiles of turbulence statistics in and above an urban street canyon. *Atmos. Environ.,* **29,** 1473–1486.

——, S.-E. Gryning, E. Batchvarova, A. Christen, and R. Vogt, 2004: Pollutant dispersion close to an urban surface—The BUBBLE tracer experiment. *Meteor. Atmos. Phys.,* **87,** 39–56.

Roth, M., and T. R. Oke, 1995: Relative efficiencies of turbulent transfer of heat mass and momentum over a patchy urban surface. *J. Atmos. Sci.,* **52,** 1863–1874.

Salmond, J. A., 2005: Wavelet analysis of intermittent turbulence in the very stable nocturnal boundary layer: Implications for the vertical mixing of ozone. *Bound.-Layer Meteor.,* **114,** 463–488.

——, M. Roth, T. R. Oke, A. N. V. Satyanarayana, and A. Christen, 2003: Comparison of turbulent fluxes from roof top versus street canyon locations using scintillometers and eddy covariance techniques. *Proc. Fifth Int. Conf. on Urban Climate (ICUC-5*), Lodz, Poland, University of Lodz, Paper O.10.3. [Available online at http://www.geo.uni.lodz.pl/~icuc5.]

Scanlon, T. M., and J. D. Albertson, 2001: Turbulent transport of carbon dioxide and water vapor within a vegetation canopy during unstable conditions: Identification of episodes using wavelet analysis. *J. Geophys. Res.,* **106** (D7), 7251–7262.

Torrence, C., and G. P. Compo, 1998: A practical guide to wavelet analysis. *Bull. Amer. Meteor. Soc.,* **79,** 61–76.

Uno, I., S. Wakamatsu, H. Ueda, and A. Nakamura, 1988: An observational study of the structure of the nocturnal urban boundary layer. *Bound.-Layer Meteor.,* **45,** 9–82.

——, ——, ——, and ——, 1992: Observed structure of the nocturnal urban boundary-layer and its evolution into a convective mixed layer. *Atmos. Environ. Part B Urban Atmos.,* **26,** 45–57.